

PCCP

Accepted Manuscript



This is an *Accepted Manuscript*, which has been through the Royal Society of Chemistry peer review process and has been accepted for publication.

Accepted Manuscripts are published online shortly after acceptance, before technical editing, formatting and proof reading. Using this free service, authors can make their results available to the community, in citable form, before we publish the edited article. We will replace this *Accepted Manuscript* with the edited and formatted *Advance Article* as soon as it is available.

You can find more information about *Accepted Manuscripts* in the [Information for Authors](#).

Please note that technical editing may introduce minor changes to the text and/or graphics, which may alter content. The journal's standard [Terms & Conditions](#) and the [Ethical guidelines](#) still apply. In no event shall the Royal Society of Chemistry be held responsible for any errors or omissions in this *Accepted Manuscript* or any consequences arising from the use of any information it contains.

Cite this: DOI: 10.1039/c0xx00000x

www.rsc.org/pccp

PAPER

Assessing the impact of anion- π effects on phenylalanine ion structures using IRMPD spectroscopy

Michael Burt, Kathleen Wilson, Rick Marta, Moaraj Hasan, W. Scott Hopkins and Terry McMahon*

Received (in XXX, XXX) Xth XXXXXXXXX 20XX, Accepted Xth XXXXXXXXX 20XX

DOI: 10.1039/b000000x

The gas-phase structures of two halide-bound phenylalanine anions (PheX⁻, X = Cl⁻ or Br⁻) and six fluorinated derivatives have been identified using infrared multiple photon dissociation (IRMPD) spectroscopy. The addition of electron-withdrawing groups to the aromatic ring creates a π -acidic system that additionally stabilizes the halide above the ring face. Detailed ion structures were determined by comparing the IRMPD spectra with harmonic and anharmonic infrared spectra computed using B3LYP/6-311++G(d,p) as well as with 298 K enthalpies and Gibbs energies determined by the MP2(full)/6-311++G(2d,2p)//B3LYP/6-31+G(d,p) and MP2(full)/aug-cc-pVTZ//B3LYP/6-31+G(d,p) methods. PheX⁻ structures were found to be dependent on both the nature of the anion and the extent of ring fluorination. Canonical isomers were established to be the dominant structures in every case, but halide addition significantly narrowed the energy gap with zwitterionic potential energy surfaces. This enabled zwitterions to appear as minor contributors to the gas-phase populations of Phe3F₂Cl⁻ and PheF₅Br⁻.

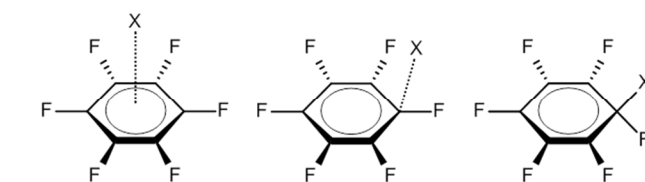
1. Introduction

Non-covalent interactions substantially affect the structures of biomolecules.¹⁻³ Prominent examples include DNA base pairing, which originates from hydrogen bonding,⁴ as well as protein folding and molecular recognition, which are controlled by π - π stacking and cation- π effects.^{5,6} Perhaps counterintuitively, it is also possible to stabilize molecules through anion- π interactions; either between the anion and the edge of an aromatic ring, or by using electron withdrawing groups to promote interactions directly with the ring face.⁷⁻⁹ The stabilizing effect of this contact, 20–70 kJ/mol, is similar to cation- π interactions or hydrogen bonds and supports expectations that anion- π interactions may be fundamentally involved in ion transport, structural control, and anion recognition.^{10,11}

Anionic interactions may also stabilize isolated amino acid zwitterions.^{12,13} These naturally adopt canonical isomers in the gas phase,^{14,15} but oxalate and malonate are computationally predicted to cluster with zwitterionic glycine,¹⁶ and halide-bound ArgX⁻ zwitterions have been confirmed by infrared multiple photon dissociation (IRMPD) spectroscopy.¹⁷ The current work similarly uses IRMPD spectroscopy to identify the structures of PheX⁻ complexes (X = Cl⁻ and Br⁻) and five fluorinated derivatives (3- and 4-fluoro, 2,5- and 3,5-difluoro, and pentafluoro). Phenylalanine is apt for further scrutiny because its nonpolar side chain and aromatic ring make it an archetype for π interactions. It therefore represents the simplest case where anion- π effects could influence the formation of gas-phase zwitterions.¹⁸

Fluorinating the ring of phenylalanine makes it possible to gauge the influence of electron withdrawing groups on anion- π interactions. The negative quadrupole moment of benzene ($\Theta_{C_6H_6}$

= $-33.3 \times 10^{-40} \text{ C}\cdot\text{m}^2$) inverts when the ring is fully substituted with fluorine ($\Theta_{C_6F_6} = 31.7 \times 10^{-40} \text{ C}\cdot\text{m}^2$). This creates a π -acidic area at the center of the ring that will influence the relative stabilities of potential halide binding sites.¹⁹ Nucleophilic anions, for example, usually form Meisenheimer σ -complexes, but establish themselves above the center of π -acidic arenes or over their peripheries in anion-donor π -acceptor configurations (Scheme 1). Charge-diffuse anions are also less likely to form σ -complexes. In the gas phase, fluoride-bound 1,3,5-trinitrobenzene is a Meisenheimer complex whereas the chloride-bound analogue places the anion further above the ring edge.²⁰



Scheme 1

Few gas-phase anion- π interactions have been reported, but thousands exist in condensed media.²¹ Many of these compete with hydrogen bonds to stabilize the anion.²² Benzamide, for example, binds tetrabutylammonium bromide above the ring where it is pulled off center by a hydrogen bond with the amide moiety.²³ In protonated pentafluoroaniline, by contrast, hydrogen bonding causes chloride to attach near the ring edge, but exchanging the ammonium group for amidinium results in chloride forming an anion- π interaction with the ring face instead.²⁴ Anion- π interactions can also stabilize systems governed by cation- π effects. A hemicyrptophane has been

developed to encapsulate zwitterions in a hydrophobic environment by using cation- π and anion- π interactions to stabilize the carboxylate and ammonium groups, respectively, of four non-proteinogenic amino acids.²⁵ Binding constants for this encapsulation were reported to be three times larger with anion- π interactions present than without.

The interplay between anion- π interactions and other non-covalent effects necessitates a determination of their influence on amino acid terminal groups. Since available information comes from condensed-phase experiments, a gas-phase technique capable of determining structural information in the absence of solvent effects is required. IRMPD spectroscopy has been extensively used to identify zwitterions stabilized by cations,²⁶⁻³⁶ and has recently confirmed nonzwitterionic isomers for GluX⁻, HisX⁻, and ProCl.^{17,37} This method, which is used here, involves irradiating an ion over a range of energies and monitoring its dissociation as a function of the impinging radiation frequency. Any observed vibrational modes are then assigned to specific functional groups of the molecule, and these conclusions are supported by comparing IRMPD spectra with computational spectra determined from electronic structure calculations. In this way, detailed ion structures can be inferred spectroscopically.

2. Methods

2.1. IRMPD Spectroscopy

Halide-bound phenylalanine anions and their derivatives were produced in the gas phase from 1:1 water/methanol solutions containing approximately 0.1 mM Phe ($\geq 97\%$, SynQuest Laboratories Inc.) and 0.1 mM NaCl or NaBr ($\geq 99\%$, Sigma Aldrich). Each solution was continuously injected at 100 $\mu\text{L}/\text{h}$ into an esquire3000 plus quadrupole ion trap mass spectrometer (Bruker Daltonics) using an electrospray ionization source (Agilent) in negative ion mode. The gas-phase ions were isolated using resonance ejection, and IRMPD spectra were acquired by irradiating the trapped ions with the infrared free electron laser (IR-FEL) at the Centre Laser Infrarouge d'Orsay (CLIO) for 400 ms at 5 cm^{-1} intervals between 900-2300 cm^{-1} .³⁸ 10 mass spectra were averaged per step. The reported spectra correspond to the IRMPD efficiency of the parent ion ($-\ln(I_{\text{parent}}/(I_{\text{parent}} + \sum I_{\text{fragments}}))$) as a function of the photon wavenumber. To increase overlap with the IR-FEL radiation, the kinetic energy of the ions was damped by collisions with 10^{-2} mbar of helium gas. This contracted their trajectories towards the center of the ion trap.

The CLIO IR-FEL beam was created from light emitted by a 44.4 MeV electron beam passed through an undulator within the optical cavity. Adjusting the gap between the periodic dipole magnets of the undulator enabled photon energies to be scanned over the mid-infrared region. The IR-FEL output was delivered to the trapped ions as a series of 9 μs macropulses emitted at 25 Hz with each macropulse comprising 600 picoscale micropulses. These pulses were then synchronized with the irradiation of the trapped ions using a fast electromechanical shutter. The average IR power for these experiments varied quadratically as a function of photon wavenumber between 800–1200 mW, reaching a maximum near the midpoint of the spectra. The laser spectral width was less than 0.5% of the selected wavenumber throughout the experimental range, and the wavelength profile was

monitored during spectral acquisitions using a monochromator coupled with a pyroelectric detector array.

2.2. Computations

Stable isomers of PheX⁻ and its derivatives were identified by a two-step process using Gaussian 09 (Revision C.01).³⁹ Energy minima were initially determined from candidate structures using B3LYP/6-311++G(d,p) density functional theory,⁴⁰ and single-point energy calculations were then performed on the optimized B3LYP geometries using MP2(full)/6-311++G(2d,2p) and MP2(full)/aug-cc-pVTZ.⁴¹⁻⁴⁴ This low-cost method efficiently retains the accuracy of the MP2 level of theory by exploiting the reliability and speed of B3LYP/6-311++G(d,p) structural optimizations for small gas-phase ions.⁴⁵⁻⁴⁷ 43-144 unique isomers were considered for each complex that varied according to the halide binding site and the amino acid backbone configuration. Particular care was taken to include Phe ion geometries similar to those previously observed or predicted in the gas phase.^{32,48,49}

The relative 298 K enthalpies and Gibbs energies of the PheX⁻ isomers were determined at both levels of theory by performing harmonic frequency calculations on the optimized B3LYP structures. MP2 thermochemistry was determined by adding B3LYP thermal correction factors to the MP2 single-point energies and is reported as MP2(full)/6-311++G(2d,2p)//B3LYP/6-311++G(d,p) or MP2(full)/aug-cc-pVTZ//B3LYP/6-311++G(d,p). As anharmonicity causes the fundamental frequencies of gas-phase amino acid complexes to be overestimated by up to 5%,^{50,51} anharmonic frequencies were also determined using B3LYP/6-311++G(d,p). This method increased the computational cost of our frequency analyses tenfold, and was therefore only performed on the subset of lowest energy isomers reported here. The B3LYP-derived harmonic and anharmonic frequencies were compared with the IRMPD spectra to assist with structural identifications and vibrational mode assignments. The presented harmonic frequencies are scaled by a factor of 0.978 to account for anharmonic effects. This value was determined by comparing the average difference between harmonic and anharmonic peak positions, and agrees with scaling factors used for similar work.^{17,38}

3. Results and Discussion

3.1. IRMPD Spectra of PheCl⁻ and the Fluorinated Complexes

The IRMPD spectrum of PheCl⁻ in the 950-1900 cm^{-1} region is compared with the spectra of five fluorinated derivatives (3- and 4-fluoro, 2,5- and 3,5-difluoro, and pentafluoro) in Figure 1. Each band stems from the loss of HCl during the IRMPD process. For PheF₅Cl⁻, this was uniquely followed by HF loss around 1504 cm^{-1} . PheF₅Br⁻, which is also compared in Figure 1, loses pentafluorophenylalanine upon absorption. PheBr⁻ was not produced with sufficient intensity to perform IRMPD.

The chloride-containing spectra are distinct, but two bands are common to each complex: a broad absorption centered between 1360-1385 cm^{-1} and a sharper peak at 1710-1740 cm^{-1} . The latter is the $\nu(\text{CO})$ stretching mode, which is red-shifted relative to the IR spectrum of gaseous phenylalanine (1779 cm^{-1}) but similar to

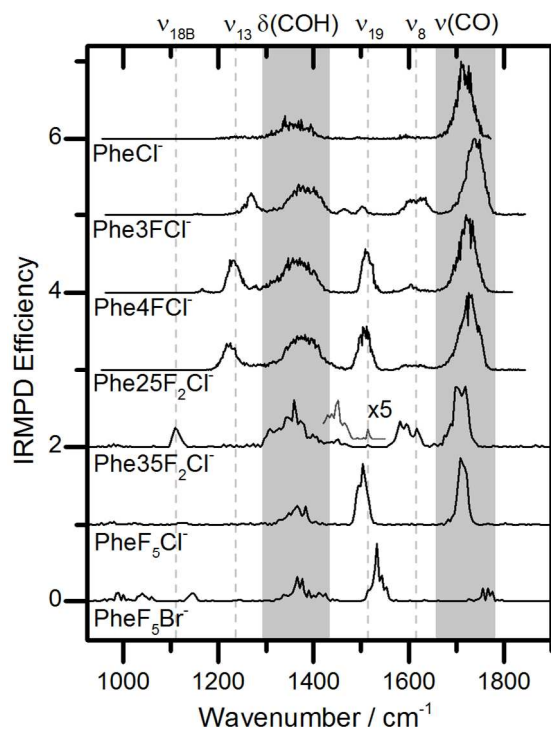
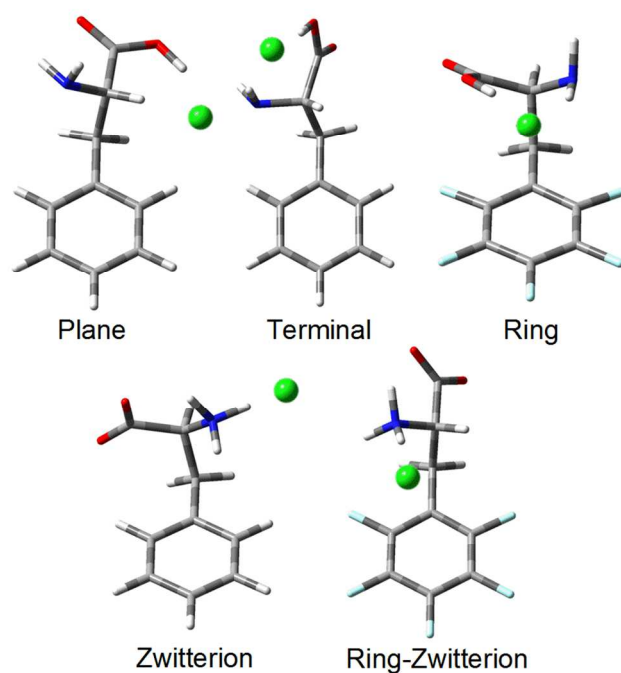


Fig. 1 IRMPD spectra of PheCl and six fluorinated PheX⁻ derivatives in the 950-1900 cm⁻¹ region.

the $\nu(\text{CO})$ absorptions of [CsPhe]⁺ (1748 cm⁻¹), [KPhe]⁺ (1745 cm⁻¹), and [AgPhe]⁺ (1729 cm⁻¹).^{26,52-54} [KPhe]⁺ and [AgPhe]⁺ bind the metal over the aromatic ring and between the nitrogen and carbonyl oxygen of a charge-solvated amino acid. Considering their similar structures, the difference in $\nu(\text{CO})$ stretching frequencies likely arises from the change in effective ionic radii between K⁺ (138 pm) and Ag⁺ (115 pm);⁵⁵ the smaller ion participates in a stronger Coulombic interaction with the carbonyl oxygen and induces a greater red shift. [CsPhe]⁺ primarily exists as a mixture of bidentate isomers, and its $\nu(\text{CO})$ mode cannot, therefore, be directly compared with the K⁺ or Ag⁺ complexes. In any case, Cl⁻ (181 pm) is larger than both Cs⁺ (167 pm) and K⁺, but the $\nu(\text{CO})$ stretching frequency of PheCl (1710 cm⁻¹) implies a stronger ion-ligand interaction energy than [AgPhe]⁺ and may indicate that PheCl adopts a different structure from those listed above. This is supported by the location of the second common band in the PheCl IRMPD spectrum (1360 cm⁻¹), which is assigned as the carboxylic hydrogen $\delta(\text{COH})$ in-plane bending mode. This absorption appears near 1400 cm⁻¹ in the IRMPD spectra of [CsPhe]⁺, [KPhe]⁺ and [AgPhe]⁺ and its red-shifted position relative to these complexes infers an interaction between Cl⁻ and the carboxylic acid. This is consistent with the observed HCl loss, which would be facilitated by this proximity.

There are several isomers other than the “ring” configurations of [KPhe]⁺ and [AgPhe]⁺ that could be adopted by PheCl and its derivatives. These include charge-solvated structures where chloride binds to the amino acid terminal groups; “plane” configurations where a terminal-bound chloride interacts with the positive edge of the aromatic ring; and zwitterionic analogues of both the ring and terminal structures. As PheCl is unlikely to form a ring structure based on its negative quadrupole moment



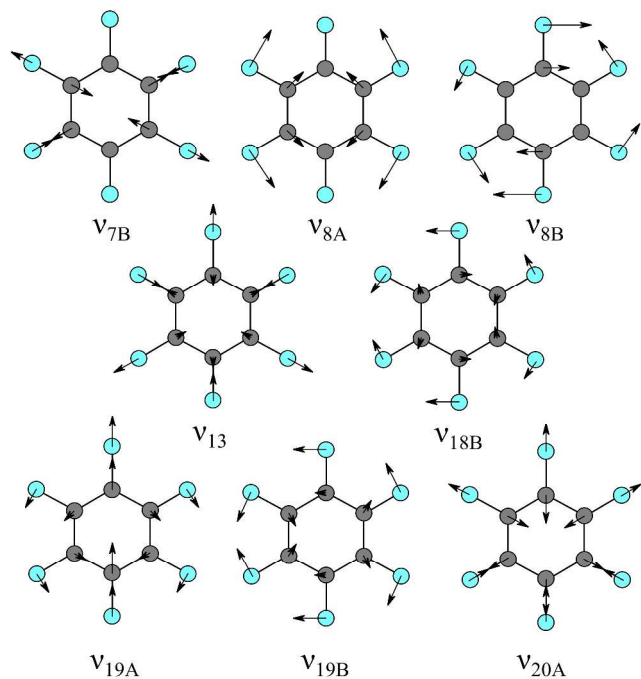
Scheme 2

and $\nu(\text{CO})$ stretching frequency, it is expected to adopt a plane or terminal structure. The latter can occur either between the carboxyl oxygens as in the case of [CsPhe]⁺, or the carbonyl oxygen and amine nitrogen.

The change in π -acidity of the fluorinated complexes may enable them to stabilize any of the isomers in Scheme 2. Their IRMPD spectra have one to four more bands than PheCl. The simplest pattern belongs to PheF₅Cl⁻, which in addition to the $\nu(\text{CO})$ and $\delta(\text{COH})$ modes exhibits a sharp band at 1504 cm⁻¹ with a possible shoulder at 1495 cm⁻¹. These are assigned to in-plane vibrations of the phenyl ring and designated ν_{19A} and ν_{19B} , respectively, as per Wilson’s notation (Scheme 3).⁵⁶ ν_{19} absorptions are diagnostic tools for identifying fluorinated benzenes.⁵⁷⁻⁵⁹ They are degenerate e_{1u} fundamental lines (1530 cm⁻¹) in the vapour- and solid-phase C₆F₆ IR spectra,^{60,61} but the loss of symmetry in C₆H_(6-n)F_n molecules creates a doublet between 1430-1540 cm⁻¹. The C₆F₅CH₃ ν_{19A} and ν_{19B} stretching modes, for example, appear at 1525 and 1510 cm⁻¹.^{62,63} and are similar for m-fluorotoluene (1492 and 1460 cm⁻¹)⁶⁴ and p-fluorotoluene (1513 and 1435 cm⁻¹).⁶⁴⁻⁶⁶ For this reason, the Phe3FCl modes at 1504 and 1465 cm⁻¹ are also attributed to ν_{19A} and ν_{19B} absorptions. The separation of the ν_{19} peaks in the Phe4FCl IRMPD spectrum (1521 and 1509 cm⁻¹), by contrast, likely represents separate ν_{19A} modes, indicating the presence of at least two isomers. The absence of related Phe4FCl ν_{19B} absorptions is consistent with the IR spectra of m- and particularly p-fluorotoluene, where a negligible cross-section for ν_{19B} is also reported.^{66,67}

The ν_{19} bands of Phe25F₂Cl⁻ and Phe35F₂Cl⁻ are more difficult

* These have been alternatively described as ν_{20} modes and vice versa, a distinction that is somewhat arbitrary given their similar motion and lack of D_{6h} symmetry.



Scheme 3

to assign. The IRMPD spectrum of the former has a broad ν_{19A} peak at 1504 cm^{-1} , whereas the latter presents a very weak ν_{19A} absorbance at 1514 cm^{-1} as well as a distinct shoulder on the $\delta(\text{COH})$ band at 1450 cm^{-1} attributed to a ν_{19B} mode.⁶⁸ The difference between the two spectra is striking; a possible explanation comes from the ν_{19} bands of *m*-difluorobenzene (1490 and 1449 cm^{-1}) and *p*-difluorobenzene (1511 and 1437 cm^{-1}).^{64,65} These are in similar positions to the peaks observed here, but, as was the case for the monofluorinated derivatives, the intensity of the lower energy absorption is significantly stronger in the *m*-difluorobenzene IR spectrum.⁵⁹

Aromatic modes between 1560 – 1650 cm^{-1} are in-plane tangential C-C ν_8 vibrations that correspond to degenerate e_{2g} lines in the C_6F_6 (1655 cm^{-1}) and C_6H_6 (1606 cm^{-1}) IR spectra. It has been reported that breaking D_{6h} symmetry causes the relative frequencies of ν_8 pairs to change with the aromatic substitution pattern.^{57,59} The calculations reported here, however, always predict ν_{8A} modes to have the higher frequency. A ν_8 pair is distinguishable in the IRMPD spectrum of Phe3FCl (1631 and 1604 cm^{-1}), but remains unresolved for Phe4FCl (1570 – 1640 cm^{-1}) and Phe25F₂Cl (1580 – 1630 cm^{-1}). The Phe35F₂Cl spectrum exhibits three absorptions (1617 , 1595 , and 1580 cm^{-1}) that likely obscure two overlapping ν_8 doublets, confirming at least two isomers exist simultaneously. It should be noted that the broad ν_8 bands of Phe4FCl and Phe25F₂Cl may also indicate the presence of more than one isomer. ν_8 separation increases as symmetry is broken; the ν_8 pair of 2,5-difluorotoluene (1627 and 1597 cm^{-1}),⁶⁸ for example, is more widely separated than those of *p*-fluorotoluene and both *m*- and *p*-difluorobenzene.^{58,64,65} This is consistent with the two ν_{19A} modes identified for Phe4FCl, as well as the broad ν_{19A} peak exhibited by Phe25F₂Cl.

Phe3FCl and Phe4FCl display sharp peaks at 1268 and 1228 cm^{-1} that are typical of monofluorinated benzenes.^{56,57} These match fluorine-sensitive ν_{13} modes of *m*-fluorotoluene (1251 cm^{-1})

¹) and *p*-fluorotoluene (1214 cm^{-1}) and are best described as in-plane C-F stretching vibrations coupled with radial skeletal vibrations of the aromatic ring.^{57,63,64} The higher energy of the Phe3FCl vibration results from the greater inductive effect of the alkyl chain on the relevant carbon atom. Phe25F₂Cl also exhibits a ν_{13} mode at 1225 cm^{-1} that is similar to the analogous vibration of 2,5-difluorotoluene (1195 cm^{-1}),⁶⁷ but the assignment of a ν_{13} band for Phe35F₂Cl is less obvious. ν_{13} absorptions have been identified up to 1350 cm^{-1} in aromatic rings substituted at the 1,3,5-positions by “light” (alkyl or fluoride) groups,⁵⁷ and the ν_{13} mode of *m*-C₆H₄F₂ suggests that the analogous Phe35F₂Cl absorption should appear near 1300 cm^{-1} .⁶⁴ There is indeed a transition at 1310 cm^{-1} that could be the ν_{13} mode, but it may also arise due to in-plane bending (ν_3) or Kekulé (ν_{14}) absorptions. Since neither was identified in the other spectra, however, we favour assignment of the 1310 cm^{-1} peak to a ν_{13} mode.

The IRMPD spectrum of Phe35F₂Cl also contains a sharp, medium intensity peak at 1109 cm^{-1} . This band is ambiguous; it likely results from in-plane bending of the aromatic ring but contributions from C-F bonds broaden the observed range of potential modes to such a degree that none are typically used for the identification of fluorinated benzenes. The band could be a consequence of ν_{9B} or ν_{18B} absorptions that appear at 1157 and 1120 cm^{-1} , respectively, for *m*-difluorobenzene.⁶⁴ Of the two, ν_{18B} is the most intense. The same mode, however, is weaker than ν_{9B} for 2,5-difluorotoluene. This is consistent with the non-observation of an analogous peak in the IRMPD spectrum of Phe25F₂Cl, and so the 1109 cm^{-1} peak is assigned as a ν_{18B} mode.⁶⁷

PheF₃Br is best compared to PheF₃Cl. Their IRMPD intensities are noticeably different, but their peak positions are similar. The $\nu(\text{CO})$ and $\delta(\text{COH})$ modes of PheF₃Br are centered at 1766 cm^{-1} and 1390 cm^{-1} as compared to 1709 cm^{-1} and 1365 cm^{-1} for PheF₃Cl. This shift can be attributed to the weaker Coulombic interaction formed by bromide (ionic radius = 196 pm). The asymmetry in the $\delta(\text{COH})$ mode is interesting in that it suggests the presence of multiple isomers. This is supported by the observation of three distinct peaks in the $\nu(\text{CO})/\nu_{as}(\text{CO}_2)$ region at 1776 , 1766 , and 1756 cm^{-1} , as well as the ν_{19} region, which exhibits a high intensity absorption at 1534 cm^{-1} as well as lower energy shoulders at 1553 , 1543 , and 1518 cm^{-1} . Since this latter absorption is expected to arise from the ν_{19} doublet, the complexity of this peak indicates more than one isomer is contributing to the gas-phase population.

The lack of comparative data makes the remaining modes more difficult to assign. The peak at 1144 cm^{-1} is $\sim 45\text{ cm}^{-1}$ higher in energy than the ν_{18B} band of Phe35F₂Cl, but cannot originate from ν_{18} or ν_9 modes because both absorb below $\sim 350\text{ cm}^{-1}$ in hexasubstituted benzenes.⁵⁸ Our calculations, however, indicate that it arises from a ν_{7B} absorption; an observation that is validated by the appearance of a ν_{7B} mode at 1153 cm^{-1} in the vapour-phase IR spectrum of $\text{C}_6\text{F}_5\text{CH}_3$.⁶³ Using the same data, as

** Aromatic C-C-H bending modes ($\nu_{9A/B}$ and $\nu_{18A/B}$) also absorb in the 1060 – 1200 cm^{-1} region, so the assigned modes originate in part from in-plane hydrogen wagging on the ring. This is consistent with the DFT results presented below.

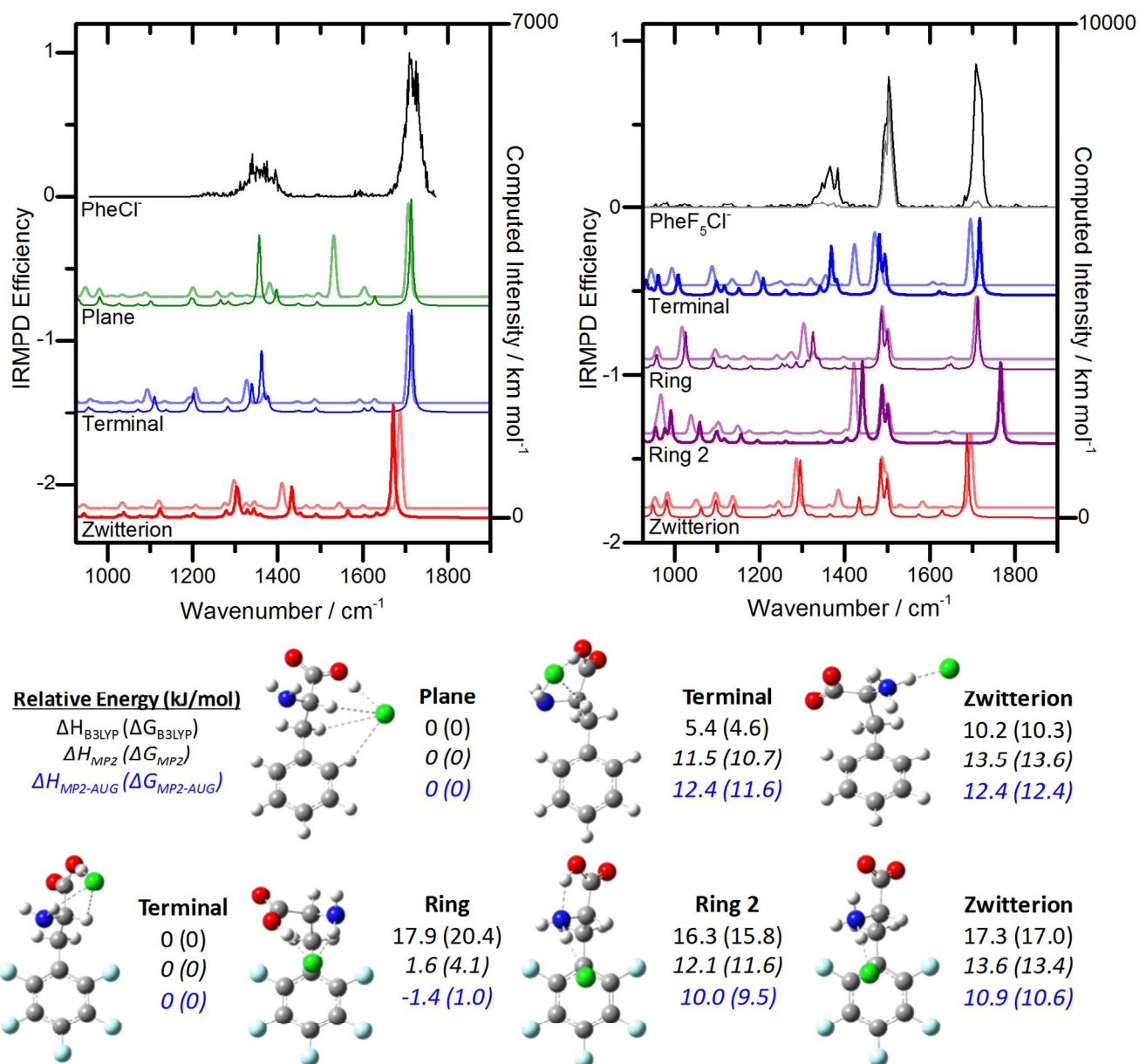


Fig. 2 The PheCl (left) and PheF₅Cl (right) IRMPD spectra (black) compared with harmonic (opaque lines) and anharmonic (transparent lines) computed IR spectra. The computed spectra are determined from the B3LYP/6-311++G(d,p) optimized structures. 298 K relative enthalpies and Gibbs energies (in parentheses) are provided at the B3LYP/6-311++G(d,p) (top), MP2(full)/6-311++G(2d,2p)//B3LYP/6-311++G(d,p) (black and italicized), and MP2(full)/aug-cc-pVTZ//B3LYP/6-311++G(d,p) (blue and italicized) levels of theory.

well as the knowledge that multiple isomers exist together, the absorptions at 1060 and 1040 cm⁻¹ are assigned to rocking motions of the phenylalanine backbone, and the peaks at 1000 and 987 cm⁻¹ are attributed to distinct ν_{20A} modes.

3.2. PheCl

The most stable predicted structures of PheCl are canonical (Figure 2). The lowest energy isomer places the chloride anion in-plane with the aromatic ring where it is stabilized through interactions with the carboxylic acid and an aromatic hydrogen. This “plane” structure is 11.6 kJ/mol lower in energy than the second canonical isomer, which binds chloride between the amine and carboxyl moieties in a “terminal” configuration. The

most stable zwitterion is 12.4 kJ/mol less favourable than the plane structure, but demonstrates that chloride stabilizes phenylalanine zwitterion formation by ~80-90 kJ/mol.⁴⁸

Figure 2 also compares the computed harmonic and anharmonic IR spectra of these isomers with the PheCl IRMPD spectrum to identify the spectral carrier. The harmonic calculations suggest PheCl is canonical; the $\nu(\text{CO})$ modes of the plane and terminal isomers (1714 and 1715 cm⁻¹) agree very well with the IRMPD spectrum. On the other hand, the predicted zwitterionic $\nu_{as}(\text{CO}_2^-)$ mode is outside the range of the 1710 cm⁻¹ peak, and the NH₃ umbrella mode expected at 1433 cm⁻¹ cannot explain the absorption centered at 1360 cm⁻¹, which, in agreement with our previous assignment, is a better match for the plane and

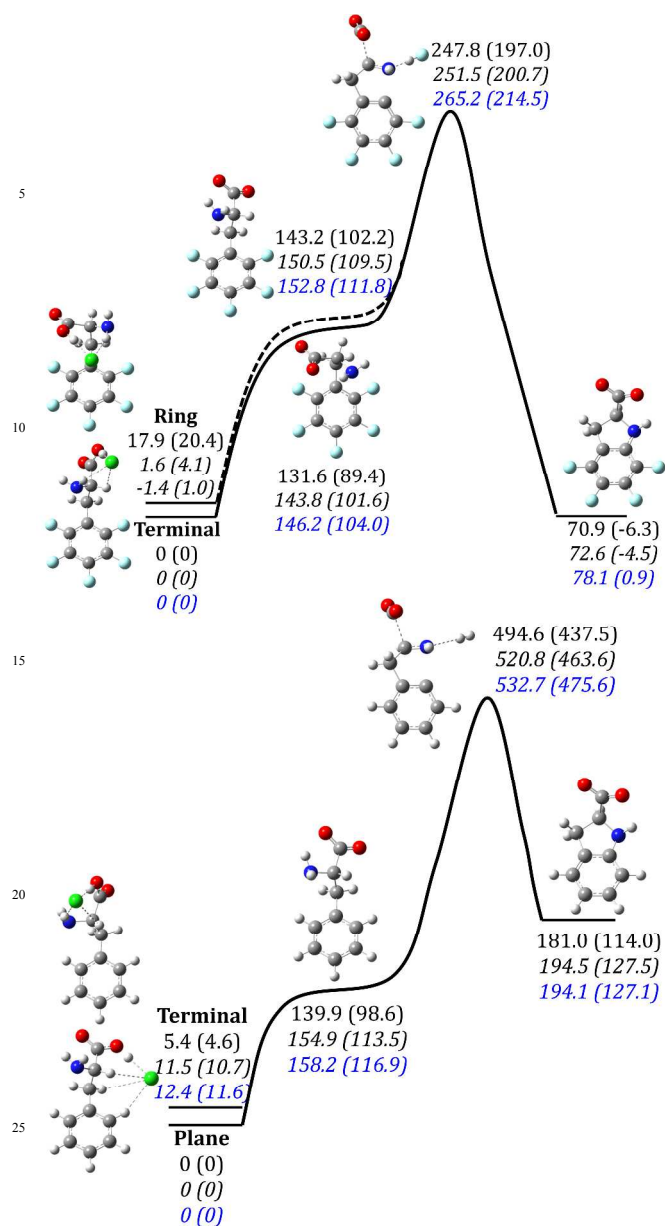


Fig. 3 The potential energy surface for the sequential loss of HCl and HF from PheF₅Cl compared with the energy required to remove HCl and H₂ from PheCl. 298 K relative enthalpies and Gibbs energies are reported as per Fig. 2 and include relevant contributions from HCl, HF, and H₂. These are listed in Table S1 of the Supporting Information.

terminal $\delta(\text{COH})$ modes predicted between 1339-1397 cm^{-1} . The anharmonic spectra of the PheCl isomers are essentially the same as their harmonic counterparts with the notable exception that the terminal isomer provides a better fit for the $\delta(\text{COH})$ absorption than the plane structure. For this reason, we assign it as the most probable structure, although the lower energy of the plane isomer, as well as its predicted harmonic spectrum, indicate that gas-phase PheCl may exist as a mixture of canonical isomers.

3.3. PheF₅Cl

Fully fluorinating the aromatic ring of phenylalanine inverts its quadrupole moment and stabilizes anions in the π -acidic region above the ring face. For this reason, the viability of PheF₅Cl

“ring” isomers must be considered. The most stable PheF₅Cl ring structure has chloride bound above the center of the ring and between the carboxyl and amine groups (Figure 2). This structure is 1.0 kJ/mol less stable than the global minimum, which is a terminal isomer, and 9.6 kJ/mol more favourable than the lowest energy zwitterion. No plane structures were identified. This is attributed to the presence of fluorine at the 2 and 6 ring positions.

The IRMPD spectrum of PheF₅Cl is compared to the computed IR spectra of the predicted isomers in Figure 2. This comparison indicates that two, possibly three, isomers coexist. Of these, the ring and terminal structures dominate and, based on their respective Gibbs energies, would have a 3:2 population ratio at 298 K. Their coexistence is supported by the enthalpic stability of the ring isomer, which is 1.4 kJ/mol more favourable than the terminal structure. There are also grounds for assigning the reproducible shoulder at 1682 cm^{-1} to the $\nu_{\text{as}}(\text{CO}_2^-)$ mode of the zwitterionic structure, which is the most stable matching isomer. The proposed $\nu(\text{CO})$ and $\nu_{\text{as}}(\text{CO}_2^-)$ modes are separated by 27 cm^{-1} , well outside the experimental bandwidth. Furthermore, the relative Gibbs energy of the zwitterion infers its intensity should be less than 2% of the $\nu(\text{CO})$ absorption. This is comparable to the relative IRMPD intensity of the $\nu_{\text{as}}(\text{CO}_2^-)$ mode, which is 8.6% as strong as the $\nu(\text{CO})$ peak. A zwitterionic structure cannot be unambiguously confirmed, however, because the predicted absorption near 1286-1295 cm^{-1} is either non-existent or too weak to be observed. A possible reason for non-observation could simply be that this peak, which arises in part from hydrogen motion between the amine nitrogen and carbonyl oxygen, results in a diffuse band due to intramolecular hydrogen bonding; a prospect that may also explain why the canonical analogue of the zwitterion (ring 2) is not observed despite being 1.1 kJ/mol more stable. Although it is not possible to confirm or eliminate the zwitterionic structure, it forms at most only a small part of the 298 K population of PheF₅Cl, which clearly exists as a mixture of ring and terminal isomers.

The PheF₅Cl IRMPD data is distinct from the other chloride-bound fluorinated derivatives in that HF dissociation was observed after the loss of HCl. This sequential dissociation (Figure 2, in gray) contributes about nine-tenths of the ν_{19} intensity. We interpret this to mean that C-F bond activation enables a fluoride to interact with a nearby proton. Since this must involve a benzylic or amine hydrogen the likely product should be a carbene or indolecarboxylate. The latter is not unusual,^{69,70} and our calculations show it to be 130.0 kJ/mol more stable than the most stable carbene (Figure S2, Supporting Information) and nearly isoenergetic with the global minimum PheF₅Cl structure (Figure 3, top). HF dissociation from (PheF₅-H) is therefore exergonic with an energy barrier of 102.7 kJ/mol for the ring isomer and 110.5 kJ/mol for the terminal isomer. The analogous loss of H₂ from (Phe-H)⁻ (Figure 3, bottom), by contrast, is endergonic by 10.2 kJ/mol and has a reaction barrier of 358.7 kJ/mol. This demonstrates that the continued dissociation of PheF₅⁻ results from fluorine ortho-substitution.

3.4. Mono- and Difluorinated Derivatives

The predicted structures of both monofluorinated phenylalanine derivatives are shown in Figure 4. In each case, the plane isomers have the lowest energy. For Phe3FCl⁻ and Phe4FCl⁻, these are 11.6 and 13.8 kJ/mol more stable than their respective terminal

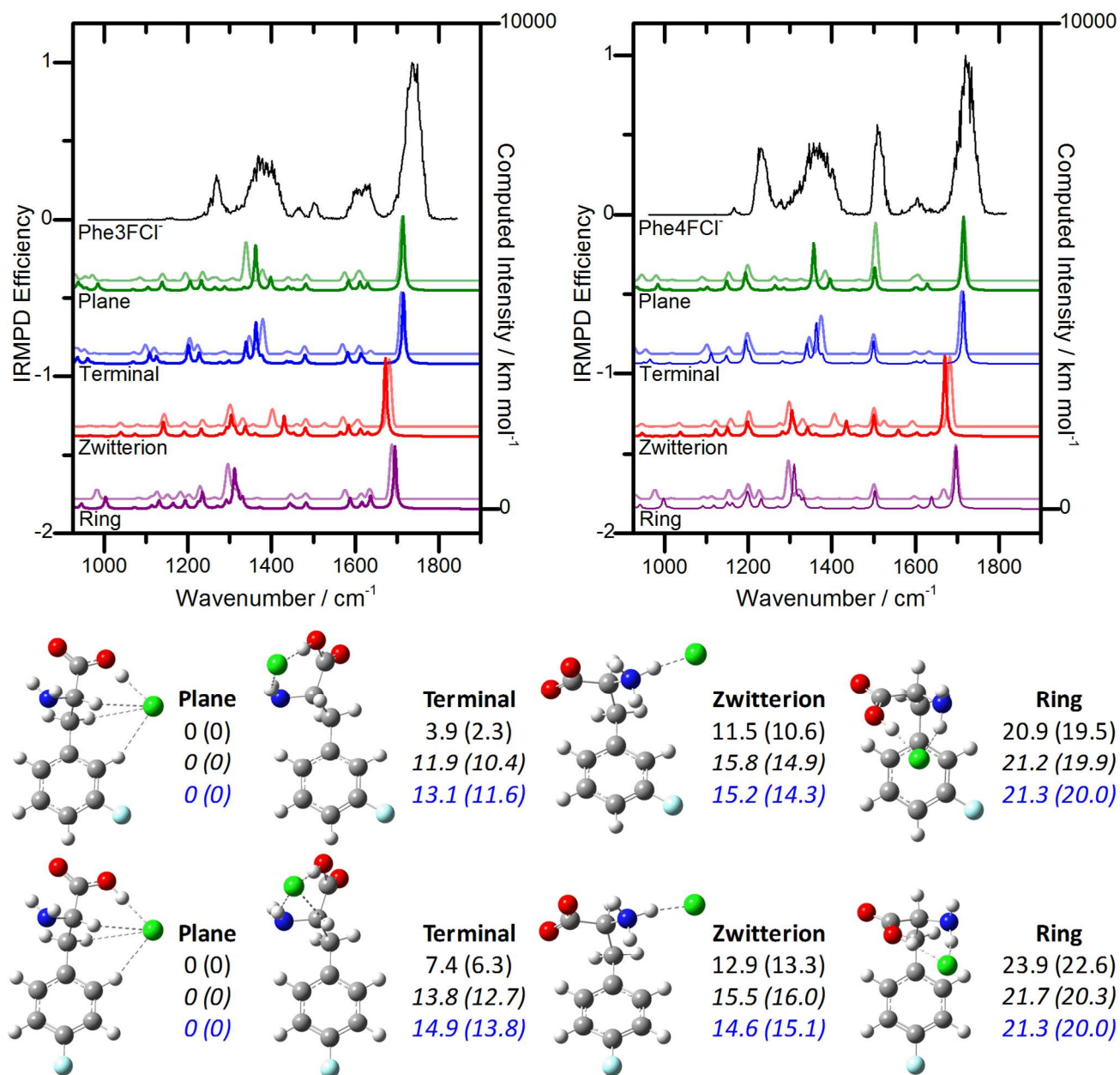


Fig. 4 The Phe3FCI⁻ (left) and Phe4FCI⁻ (right) IRMPD spectra (black) compared with harmonic (opaque lines) and anharmonic (transparent lines) computed IR spectra. The computed spectra are determined from the B3LYP/6-311++G(d,p) optimized structures. 298 K relative enthalpies and Gibbs energies (in parentheses) are provided at the B3LYP/6-311++G(d,p) (top), MP2(full)/6-311++G(2d,2p)//B3LYP/6-311++G(d,p) (black and italicized), and MP2(full)/aug-cc-pVTZ//B3LYP/6-311++G(d,p) (blue and italicized) levels of theory

isomers, 14.3 and 15.1 kJ/mol more favourable than the lowest energy zwitterions, and 20.0 kJ/mol more stable than both ring structures. This trend is more like the PheCl⁻ rather than the PheF₅Cl⁻ case in that the relative energies of the zwitterions are lower than those of the ring structures. This result is reasonable; since less electron density is withdrawn from the ring it becomes more difficult to stabilize chloride above it.

Figure 4 also compares the harmonic and anharmonic IR spectra of the computed structures with their corresponding IRMPD spectra. For Phe3FCI⁻, the intense bands at 1738 cm⁻¹ and 1385 cm⁻¹ indicate that plane and terminal isomers dominate the spectrum. Zwitterionic or ring structures cannot be eliminated,

however, because the $\nu(\text{CO})$ band is broader than in the PheCl⁻ spectrum and has a shoulder at 1699 cm⁻¹. The $\delta(\text{COH})$ mode is also asymmetric around 1320 cm⁻¹, a feature that, according to our calculations, can only arise from these higher energy isomers. The presence of multiple isomers is clearer in the case of Phe4FCI⁻. The Phe3FCI⁻ and Phe4FCI⁻ IRMPD spectra are significantly different around 1500 cm⁻¹. In the former, the doublet at 1504 and 1465 cm⁻¹ originates from $\nu_{19\text{A}}$ and $\nu_{19\text{B}}$ stretching modes, but the peak at 1509 and shoulder at 1521 cm⁻¹ in the Phe4FCI⁻ spectrum are distinct $\nu_{19\text{A}}$ absorptions, indicating at least two isomers are present. The most probable gas-phase Phe4FCI⁻ isomers are the plane and terminal canonical structures.

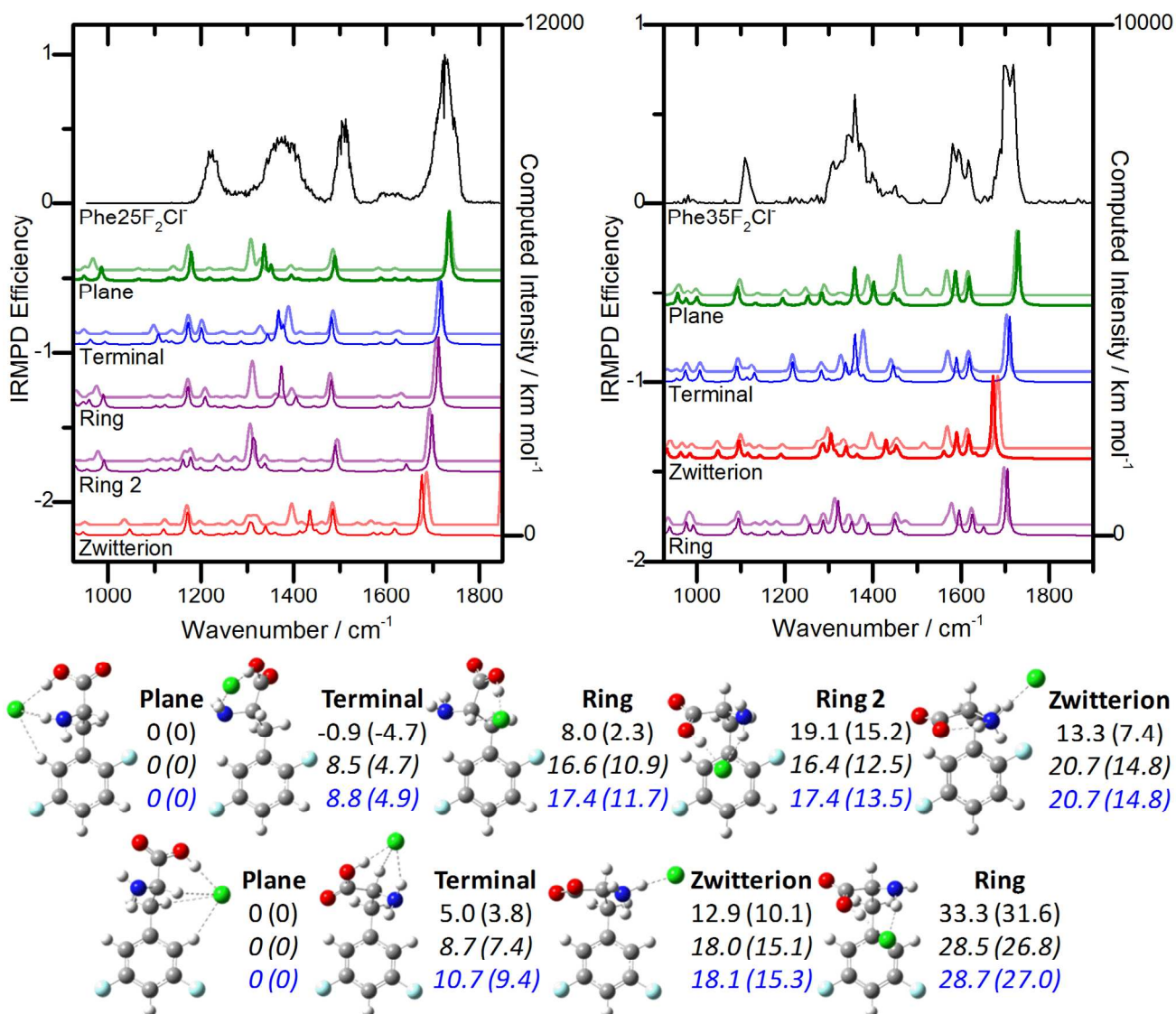


Fig. 5 The Phe25F₂Cl⁻ (left) and Phe35F₂Cl⁻ (right) IRMPD spectra (black) compared with harmonic (opaque lines) and anharmonic (transparent lines) computed IR spectra. The computed spectra are determined from the B3LYP/6-311++G(d,p) optimized structures. 298 K relative enthalpies and Gibbs energies (in parentheses) are provided at the B3LYP/6-311++G(d,p) (top), MP2(full)/6-311++G(2d,2p)//B3LYP/6-311++G(d,p) (black and italicized), and MP2(full)/aug-cc-pVTZ//B3LYP/6-311++G(d,p) (blue and italicized) levels of theory.

The $\delta(\text{COH})$ absorption profile, however, has a shoulder centered at 1279 cm⁻¹ that may infer additional minor contributions from zwitterionic or ring structures. Chloride-bound monofluorinated phenylalanine derivatives do not, therefore, have unique structures in the gas phase, but canonical plane or terminal isomers plainly overshadow the rest.

The computed structures of Phe25F₂Cl⁻ and Phe35F₂Cl⁻ are shown in Figure 5. The most stable structure for both derivatives is the plane isomer; these are 4.9 and 9.4 kJ/mol more stable than their respective terminal isomers. The relative energies of the zwitterionic and ring structures, however, follow opposing trends. The lowest energy ring and zwitterionic Phe25F₂Cl⁻ isomers are 11.7 and 14.8 kJ/mol higher in energy than the global minimum structure, but the same isomers for Phe35F₂Cl⁻ differ from the most stable structure by 27.0 and 15.3 kJ/mol; a change that can only be attributed to the fluorine substitution pattern. This is

supported by natural bond order analyses (Figure S3 in the Supporting Information),⁶⁹ which demonstrate that the aromatic carbons nearest to the chloride are more positive for Phe25F₂Cl⁻ than for Phe35F₂Cl⁻.

The IRMPD spectra of the difluorinated complexes are compared with the predicted harmonic and anharmonic IR spectra of these isomers in Figure 5. No Phe25F₂Cl⁻ structures can be ruled out spectroscopically, but based on energetics the most probable structures are canonical. Contributors to the Phe35F₂Cl⁻ spectrum, however, are easier to distinguish. The band centered at 1715 cm⁻¹ comprises two intense blended $\nu(\text{CO})$ modes at 1719 and 1702 cm⁻¹, and a $\nu_{\text{as}}(\text{CO}_2^-)$ shoulder at 1688 cm⁻¹. Based on anharmonic band positions the strong $\nu(\text{CO})$ absorptions can be attributed to the plane (1727 cm⁻¹) and terminal (1709 cm⁻¹) isomers, respectively, while the shoulder at 1688 cm⁻¹ may account for the $\nu(\text{CO})$ absorption of the ring isomer (1698 cm⁻¹)

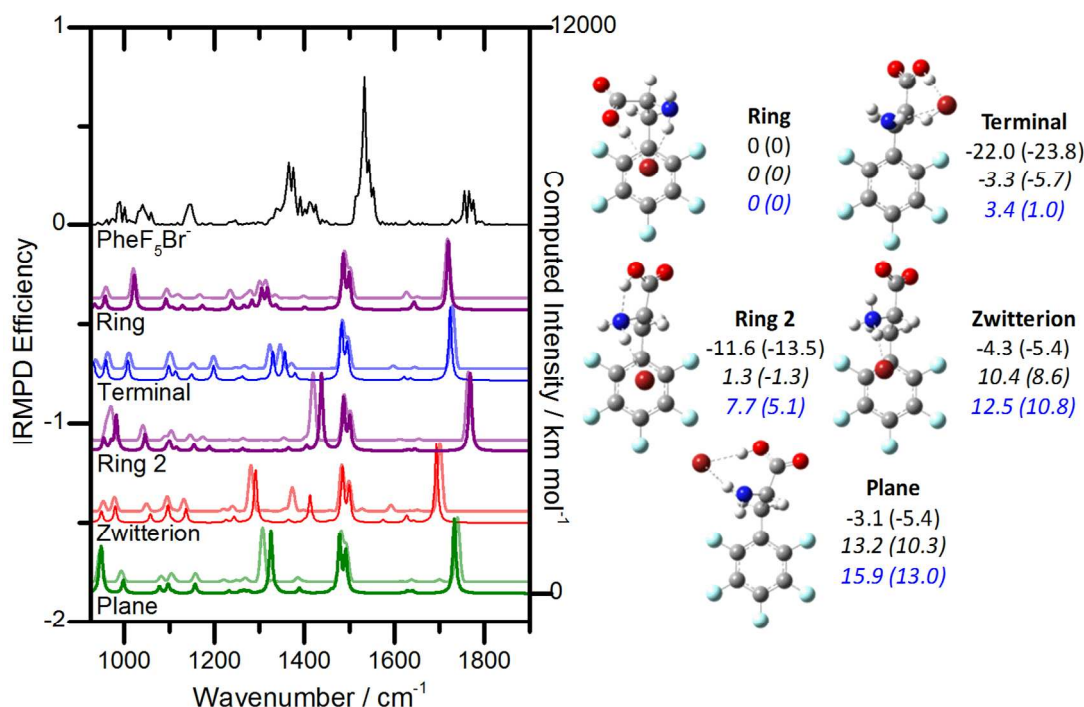


Fig. 6 The PheF_5Br^- IRMPD spectrum (black) compared with harmonic (opaque lines) and anharmonic (transparent lines) computed IR spectra. The computed spectra are determined from B3LYP/6-311++G(d,p) optimized structures. 298 K relative enthalpies and Gibbs energies (in parentheses) are provided at the B3LYP/6-311++G(d,p) (top), MP2(full)/6-311++G(2d,2p)//B3LYP/6-311++G(d,p) (black and italicized), and MP2(full)/aug-cc-pVTZ//B3LYP/6-311++G(d,p) (blue and italicized) levels of theory.

or the zwitterionic $\nu_{\text{as}}(\text{CO}_2^-)$ mode (1684 cm^{-1}). Further evidence for the existence of multiple isomers comes from the ν_8 and $\delta(\text{COH})$ regions. The former should be a doublet, so the presence of at least three separate absorptions confirms the presence of more than one isomer. The latter has several distinct peaks that, according to the calculated harmonic and anharmonic spectra, arise from a mixture of plane, terminal, ring and zwitterionic structures. The best match comes from the predicted spectra of the terminal isomer, but the peaks at 1403 and 1450 cm^{-1} agree very well with the anharmonic spectrum of the plane isomer, while the peak at 1310 cm^{-1} , earlier assigned to a ν_{13} mode, could originate from either the Kekulé ν_{14} mode of the ring isomer (1313 cm^{-1}) or the ν_{13} mode of the zwitterionic structure (1298 cm^{-1}); the latter being more likely due to its lower energy and better spectral overlap with the peak at 1688 cm^{-1} .

3.5. PheF_5Br^-

The relative energies of the PheF_5Cl^- and PheF_5Br^- isomers (Figure 6) are different, indicating that the structure of PheF_5X^- complexes is anion-dependent. For PheF_5Br^- , the most stable isomer is a ring structure that is 1.0 kJ/mol lower in Gibbs energy than the terminal structure; the opposite is true for PheF_5Cl^- . This may indicate that Br^- , which is more charge diffuse than Cl^- , stabilizes the η^6 π -interaction. It should be noted, however, that B3LYP/6-311++G(d,p) and MP2(full)/6-311++G(2d,2p)//B3LYP/6-311++G(d,p) calculations each predict the terminal isomer to be the most stable, and so it is probable that both exist in the gas phase in similar numbers. Zwitterionic and plane structures were also identified for PheF_5Br^- ; these are 10.8 and 13.0 kJ/mol , respectively, higher in energy than the ring structure.

The predicted harmonic and anharmonic IR spectra of these isomers are compared with the PheF_5Br^- IRMPD spectrum in Figure 6. The best matches according to both sets of calculated spectra come from the ring and terminal structures, although it should be noted that anharmonic effects appear to be overestimated in this case. Our spectral data suggests no scaling is necessary, but Figure 6 retains the 0.978 factor for consistency with the other presented spectra. Thermochemistry predicts that the ring and terminal isomers exist in a $3:2$ ratio at 298 K and dominate nearly the whole of the gas-phase population. Anion- π interactions, therefore, can be stabilized in the gas phase using electron withdrawing groups. The IRMPD spectrum also contains evidence of a second ring structure that is 5.1 kJ/mol higher in Gibbs energy than the most stable isomer. A zwitterionic version of this structure is only 5.7 kJ/mol less stable, and evidence for both configurations can be seen in the spectrum. There are, for example, three distinct $\nu(\text{CO})/\nu_{\text{as}}(\text{CO}_2^-)$ absorptions at 1776 , 1766 , and 1756 cm^{-1} as well as a weak absorption at 1726 cm^{-1} . The first of these is best fit by the second ring structure, while the weakest mode may belong to its zwitterionic analogue. The calculated anharmonic spectra of the zwitterionic structure also fits the lowest and highest energy $\delta(\text{COH})$ regions, indicating that part of this absorption originates from an umbrella $\delta(\text{NH}_3^+)$ moiety. A small part of the gas-phase PheF_5Br^- population can therefore be attributed to zwitterionic isomers.

3.6. Anion- π stabilization of zwitterionic structures

Gas-phase PheX^- derivatives are primarily canonical. Terminal isomers are generally the most probable structure under π -basic

conditions, while ring configurations contribute significantly to π -acidic derivatives, such as PheF_3Cl^- and PheF_3Br^- . The same trend holds for zwitterionic isomers (Table 1). The most stable zwitterionic isomers of PheF_3Cl^- and PheF_3Br^- are anion- π stabilized and are 15.4 and 17.6 kJ/mol more favourable than the lowest energy zwitterionic structures without this interaction. This latter configuration, however, is favoured by the more π -basic derivatives; the anion- π stabilized “ring-zwitterion” isomers of $\text{Phe25F}_2\text{Cl}^-$ and $\text{Phe35F}_2\text{Cl}^-$ are 12.4 and 15.0 kJ/mol less stable than zwitterionic isomers without this interaction, and no ring-zwitterions were identified for the most π -basic ions: PheCl^- , Phe3FCl^- and Phe4FCl^- . Anion- π interactions therefore stabilize zwitterions in a similar manner to canonical isomers, but this stabilization is not sufficient to replace the canonical structures as the dominant contributors to the spectra.

Table 1 Anion- π stabilization of zwitterionic structures

Complex	Isomer Energy(kJ/mol) ^a	
	Zwitterion	Ring-Zwitterion
PheCl^-	12.4	-
Phe3FCl^-	14.3	-
Phe4FCl^-	15.1	-
$\text{Phe25F}_2\text{Cl}^-$	14.8	27.2
$\text{Phe35F}_2\text{Cl}^-$	15.3	30.3
PheF_3Cl^-	26.0	10.6
PheF_3Br^-	28.4	10.8

^a Gibbs energy relative to the most stable structure determined using MP2(full)/aug-cc-pVTZ//B3LYP/6-311++G(d,p)

4. Conclusions

Interrogating the gas-phase structures of PheCl^- and six fluorinated PheX^- derivatives by IRMPD spectroscopy identified multiple isomers for each complex. In every case, these mixtures are dominated by canonical isomers, but zwitterions appear as minor contributors to the spectra of $\text{Phe35F}_2\text{Cl}^-$ and PheF_3Br^- , and cannot be ruled out for the rest. PheCl^- , Phe3FCl^- , Phe4FCl^- , $\text{Phe25F}_2\text{Cl}^-$ and $\text{Phe35F}_2\text{Cl}^-$ are best described as mixtures of plane and terminal isomers; PheF_3Cl^- and PheF_3Br^- comprise both terminal and ring structures. These isomers cannot always be separated spectroscopically, but their relative stabilities are significantly influenced by the extent of ring fluorination. Plane isomers, for example, produce the lowest energy structures for PheCl^- as well as both the mono- and difluorinated derivatives, but were not identified for PheF_3Cl^- and were the least stable for PheF_3Br^- . Ring isomers, by contrast, become more stable with increasing fluorination and are expected to make significant contributions to the gas-phase populations of PheF_3Cl^- and PheF_3Br^- .

These trends reveal that gas-phase anion- π effects become more prominent with increasing fluorination, a fact that can be explained by the corresponding increase in π -acidity. It is also clear that anion- π effects influence the relative stabilities of competing zwitterionic structures. The lowest energy zwitterions of PheF_3Cl^- and PheF_3Br^- , for example, have the anion above the center of the ring and interacting with an NH_3^+ moiety. In the case of PheF_3Br^- this stabilizing effect is sufficient to produce an observable population of gas-phase zwitterions. In all other cases, however, the most stable zwitterions exhibit no interaction with the ring.

Acknowledgements

We thank the CLIO team for their expertise and technical assistance, and gratefully acknowledge financial support from the Natural Sciences and Engineering Research Council (NSERC) of Canada as well as computational support from the SHARCNET consortium of Compute Canada.

Notes and references

Department of Chemistry, University of Waterloo, 200 University Avenue West, Waterloo, Ontario, Canada, N2L 3G1.

E-mail: mcmahon@uwaterloo.ca

[†] Electronic Supplementary Information (ESI) available: Larger versions of the structures discussed in this article are shown in Figure S1 along with the bond lengths of any predicted anion-hydrogen or intramolecular hydrogen bonds; the carbene product for the sequential removal of HCl and HF can be found in Figure S2; and the results of natural bond order analyses on the ring isomers of $\text{Phe25F}_2\text{Cl}^-$ and $\text{Phe35F}_2\text{Cl}^-$ are reported in Figure S3. See DOI: 10.1039/b000000x/

- H.-J. Schneider, *Angew. Chem. Int. Ed.*, 2009, **48**, 3924-3977.
- J. Černý and P. Hobza, *Phys. Chem. Chem. Phys.*, 2007, **9**, 5291-5303.
- E. Frieden, *J. Chem. Educ.*, 1975, **52**, 754-761.
- J. D. Watson and F. H. C. Crick, *Nature*, 1953, **171**, 737-738.
- J. P. Gallivan and D. A. Dougherty, *Proc. Natl. Acad. Sci. USA*, 1999, **96**, 9459 - 9464.
- G. B. McGaughey, M. Gagné and A. K. Rappé, *J. Biol. Chem.*, 1998, **273**, 15458-15463.
- H. T. Chifotides and K. R. Dunbar, *Acc. Chem. Res.*, 2013, **46**, 894 - 906.
- A. Frontera, P. Gamez, M. Mascal, T. J. Mooibroek and J. Reedijk, *Angew. Chem. Int. Ed.*, 2011, **50**, 9564-9583.
- D.-X. Wang and M.-X. Wang, *J. Am. Chem. Soc.*, 2013, **135**, 892 - 897.
- S. Chakravarty, Z.-Z. Sheng, B. Iverson and B. Moore, *FEBS Lett.*, 2012, **586**, 4180-4185.
- M. Wenzel, J. R. Hiscock and P. A. Gale, *Chem. Soc. Rev.*, 2012, **41**, 480-520.
- E. M. Milner, M. G. D. Nix and C. E. H. Dessent, *J. Phys. Chem. A*, 2012, **116**, 801-809.
- G. Yang, Y. Zu, C. Liu, Y. Fu and L. Zhou, *J. Phys. Chem. B*, 2008, **112**, 7104-7110.
- S. Bianco, A. Lesarri, J. C. López and J. Alonso, *J. Am. Chem. Soc.*, 2004, **126**, 11675-11683.
- C. J. Chappo, J. B. Paul, R. A. Provencal, K. Roth and R. J. Saykally, *J. Am. Chem. Soc.*, 1998, **120**, 12956-12957.
- S. R. Kass, *J. Am. Chem. Soc.*, 2005, **127**, 13098-13099.
- J. T. O'Brien, J. S. Prell, G. Berden, J. Oomens and E. R. Williams, *Int. J. Mass Spectrom.*, 2010, **297**, 116-123.
- A. Gapeev and R. C. Dunbar, *J. Am. Chem. Soc.*, 2001, **123**, 8360 - 8365.
- J. Vrbancich and G. L. D. Ritchie, *J. Chem. Soc. Farad. Trans. 2*, 1980, **76**, 648-659.
- B. Chiavarino, M.-E. Crestoni, P. Maître and S. Fornarini, *Int. J. Mass Spectrom.*, 2013, **354-355**, 62-69.
- P. Vivek, J. Harris, R. Adams, D. Nguyen, J. Spiers, J. Baudry, E. E. Howell and R. J. Hinde, *Biochemistry*, 2011, **50**, 2939-2950.
- D. Escudero, A. Frontera, D. Quiñero and P. M. Deyà, *J. Comput. Chem.*, 2008, **30**, 75-82.
- M. Giese, M. Albrecht, T. Krappitz, M. Peters, V. Gossen, G. Raabe, A. Valkonen and K. Rissanen, *Chem. Commun.*, 2012, **48**, 9983-9985.
- M. Albrecht, C. Wessel, M. de Groot, K. Rissanen and A. Lüchow, *J. Am. Chem. Soc.*, 2008, **130**, 4600-4601.
- O. Perraud, V. Rovert, H. Gornitzka, A. Martinez and J.-P. Dutasta, *Angew. Chem. Int. Ed.*, 2012, **51**, 504-508.
- N. C. Polfer and J. Oomens, *Mass Spectrom. Rev.*, 2009, **28**, 468-494.

27. M. B. Burt and T. D. Fridgen, *Eur. J. Mass Spectrom.*, 2012, **18**, 235-250.
28. R. Wu, R. A. Marta, J. K. Martens, K. R. Eldridge and T. B. McMahon, *J. Am. Soc. Mass Spectrom.*, 2011, **22**, 1651-1659.
29. C. G. Atkins, K. Rajabi, E. A. L. Gillis and T. D. Fridgen, *J. Phys. Chem. A*, 2008, **112**, 10220-10225.
30. R. Wu and T. B. McMahon, *J. Am. Chem. Soc.*, 2007, **129**, 4864-4865.
31. X. Kong, I.-A. Tsai, S. Sabu, C.-C. Han, Y. T. Lee, H.-C. Chang, S.-Y. Tu, A. H. Kung and C.-C. Wu, *Angew. Chem. Int. Ed.*, 2006, **45**, 4130-4134.
32. N. C. Polfer, J. Oomens, D. T. Moore, G. von Helden, G. Meijer and R. C. Dunbar, *J. Am. Chem. Soc.*, 2006, **128**, 517-525.
33. M. K. Drayß, P. B. Armentrout, J. Oomens and M. Schäfer, *Int. J. Mass Spectrom.*, 2010, 297, 18-27.
34. M. F. Bush, J. T. O'Brien, J. S. Prell, R. J. Saykally and E. R. Williams, *J. Am. Chem. Soc.*, 2007, **129**, 1612-1622.
35. M. F. Bush, J. Oomens, R. J. Saykally and E. R. Williams, *J. Am. Chem. Soc.*, 2008, **130**, 6463-6471.
36. T. D. Fridgen, *Mass Spectrom. Rev.*, 2009, **28**, 586-607.
37. J. Schmidt and S. R. Kass, *J. Phys. Chem. A*, 2013, **117**, 4863-4869.
38. L. MacAleese, A. Simon, T. B. McMahon, J.-M. Ortega, D. Scuderi, J. Lemaire and P. Maître, *Int. J. Mass Spectrom.*, 2006, **249-250**, 14-20.
39. M. J. Frisch, G. W. Trucks, H. B. Schlegel, G. E. Scuseria, M. A. Robb, J. R. Cheeseman, G. Scalmani, V. Barone, B. Mennucci, G. A. Petersson, H. Nakatsuji, M. Caricato, X. Li, H. P. Hratchian, A. F. Izmaylov, J. Bloino, G. Zheng, J. L. Sonnenberg, M. Hada, M. Ehara, K. Toyota, R. Fukuda, J. Hasegawa, M. Ishida, T. Nakajima, Y. Honda, O. Kitao, H. Nakai, T. Vreven, J. J. A. Montgomery, J. E. Peralta, F. Ogliaro, M. Bearpark, J. J. Heyd, E. Brothers, K. N. Kudin, V. N. Staroverov, T. Keith, R. Kobayashi, J. Normand, K. Raghavachari, A. Rendell, J. C. Burant, S. S. Iyengar, J. Tomasi, M. Cossi, N. Rega, J. M. Millam, M. Klene, J. E. Knox, J. B. Cross, V. Bakken, C. Adamo, J. Jaramillo, R. Gomperts, R. E. Stratmann, O. Yazyev, A. J. Austin, R. Cammi, C. Pomelli, J. W. Ochterski, R. L. Martin, K. Morokuma, V. G. Zakrzewski, G. A. Voth, P. Salvador, J. J. Dannenberg, S. Dapprich, A. D. Daniels, O. Farkas, J. B. Foresman, J. V. Ortiz, J. Cioslowski and D. J. Fox, *Gaussian 09, Revision C.01*; Gaussian, Inc.: Wallingford, CT, 2010.
40. A. D. Becke, *J. Chem. Phys.*, 1993, **98**, 5648-5652.
41. C. Møller and M. S. Plesset, *Phys. Rev.*, 1934, **46**, 618-622.
42. M. Head-Gordon, J. A. Pople and M. J. Frisch, *Chem. Phys. Lett.*, 1988, **153**, 503-506.
43. R. A. Kendall, T. H. J. Dunning and R. J. Harrison, *J. Chem. Phys.*, 1992, **96**, 6796-6806.
44. E. R. Davidson, *Chem. Phys. Lett.*, 1996, **260**, 514-518.
45. A. P. Scott and L. Radom, *J. Phys. Chem.*, 1996, **100**, 16502-16513.
46. R. A. Marta, R. Wu, K. R. Eldridge, J. K. Martens and T. B. McMahon, *Phys. Chem. Chem. Phys.*, 2010, **12**, 3431-3442.
47. S. M. Martens, R. A. Marta, J. K. Martens and T. B. McMahon, *J. Phys. Chem. A*, 2011, **115**, 9837-9844.
48. L. C. Snoek, E. G. Robertson, R. T. Kroemer and J. P. Simons, *Chem. Phys. Lett.*, 2000, **321**, 49-56.
49. G. von Helden, I. Compagnon, M. N. Blom, M. Frankowski, U. Erlekam, J. Oomens, B. Brauer, R. B. Gerber and G. Meijer, *Phys. Chem. Chem. Phys.*, 2008, **10**, 1248-1256.
50. D. A. Clabo, Jr., W. D. Allen, R. B. Remington, Y. Yamaguchi and H. F. I. Schaefer, *Chem. Phys.*, 1988, **123**, 187-239.
51. V. Barone, *J. Chem. Phys.*, 2005, **122**, 014108.
52. R. Linder, M. Nispel, T. Häber and K. Kleinermanns, *Chem. Phys. Lett.*, 2005, **409**, 260-264.
53. N. C. Polfer, B. Paizs, L. C. Snoek, I. Compagnon, S. Suhai, G. Meijer, G. Von Helden and J. Oomens, *J. Am. Chem. Soc.*, 2005, **127**, 8571-8579.
54. R. C. Dunbar, J. D. Steill and J. Oomens, *Phys. Chem. Chem. Phys.*, 2010, **12**, 13383-13393.
55. R. D. Shannon, *Acta Cryst.*, 1976, **A32**, 751-767.
56. E. B. J. Wilson, *Phys. Rev.*, 1934, **45**, 706-714.
57. I. K. Korobeinicheva, O. M. Fugaeva and G. G. Furin, *J. Fluor. Chem.*, 1990, **46**, 179-209.
58. G. Varsányi, Assignments for vibrational spectra of seven hundred benzene derivatives, Adam Hilger Ltd., London, 1974.
59. L. M. Sverdlov, M. A. Kovner and E. P. Krainov, *Vibrational Spectra of Polyatomic Molecules*, John Wiley & Sons, Inc., New York, 1974.
60. J. D. Lapsa and C. Montgomery, *Spectrochim. Acta*, 1982, **38A**, 1109-1113.
61. D. Steele and D. H. Whiffen, *Trans. Farad. Soc.*, 1959, **55**, 369-376.
62. S. G. Frankiss and D. J. Harrison, *Spectrochim. Acta*, 1975, **31A**, 1839-1864.
63. R. T. Bailey and S. G. Hasson, *Spectrochim. Acta*, 1969, **25A**, 467-473.
64. J. H. S. Green, *Spectrochim. Acta*, 1969, **26A**, 1523-1533.
65. J. H. S. Green, *Spectrochim. Acta*, 1970, **26A**, 1503-1513.
66. E. E. Ferguson, R. L. Hudson, J. R. Nielsen and D. C. Smith, *J. Chem. Phys.*, 1953, **21**, 1736-1740.
67. S.E. Stein "Infrared Spectra" in NIST Chemistry WebBook, NIST Standard Reference Database Number 69, Eds. P.J. Linstrom and W.G. Mallard, National Institute of Standards and Technology, Gaithersburg MD, 20899, <http://webbook.nist.gov>, (retrieved December 4, 2013).
68. J. H. S. Green, D. J. Harrison and W. Kynaston, *Spectrochim. Acta*, 1971, **27A**, 807-815.
69. E. D. Glendening, J. K. Badenhop, A. E. Reed, J. E. Carpenter, J. A. Bohmann, C. M. Morales and F. Weinhold, *NBO 5.9*; Theoretical Chemistry Institute, University of Wisconsin: Madison, Wisconsin, 2009. <http://www.chem.wisc.edu/~nbo5>.
70. M. Lorion, É. Deniau, A. Couture and P. Grandclaoudon, *Sci. Stud. Res.*, 2009, **10**, 129-136.
71. M. R. Paleo, L. Castedo, D. Dominguez, *J. Org. Chem.*, 1993, **58**, 2763-2767.